Applied Catalysis B: Environmental 91 (2009) 204–209

Contents lists available at ScienceDirect

Applied Catalysis B: Environmental

journal homepage: www.elsevier.com/locate/apcatb

Promoting effect of Ce added to metal oxide supported on Al pillared clays for deep benzene oxidation

Shufeng Zuo [a,b], Qinqin Huang [a], Jing Li [a], Renxian Zhou [a,*]

[a] Institute of Catalysis, Zhejiang University, Hangzhou 310028, PR China
[b] Institute of Applied Chemistry, Shaoxing University, Shaoxing 312000, PR China

ARTICLE INFO

Article history:
Received 16 February 2009
Received in revised form 4 May 2009
Accepted 22 May 2009
Available online 27 May 2009

Keywords:
Pillared clay
Transition metal
Cerium
Redox property
Benzene oxidation

ABSTRACT

Al pillared clays (Al-PILC) were used to support transition metals (M = Cr, Mn, Fe, Co, Ni and Cu) and Ce for the deep oxidation of low concentration of benzene. The effect of Ce addition to M/Al-PILC was also investigated. The catalysts were characterized by X-ray powder diffraction, N_2 adsorption and H_2 temperature programmed reduction techniques. Introduction of Ce into M/Al-PILC improves dispersion of transition metals, changes the redox properties of metal oxide and makes it easier to be reduced by the interaction between the two oxides, increasing lattice oxygen lability. In activity tests Mn based catalysts were observed to be the most active among the transition metals, and adding Ce obviously improved the activity and stability of M/Al-PILC. Moreover, Ce content had a great effect on the activity of MnCe/Al-PILC. MnCe (18:1)/Al-PILC exhibited the highest activity, and the temperature for complete benzene conversion using this catalyst was about 310 °C.

1. Introduction

Over the last few years environmental legislation has imposed increasingly stringent targets for permitted levels of atmospheric emission. Volatile organic compounds (VOCs), present at low concentrations in industrial gas exhaust streams, are considered as significant atmospheric pollutants due to their toxicity or malodorous nature, as well as due to their contribution in smog formation. The catalytic oxidation of these pollutants to carbon dioxide and water has been identified as one of the most efficient ways to destroy VOCs at low concentrations and to meet increasingly environmental regulations [1]. Therefore, highly active catalysts at low temperatures are required. Supported precious metals such as Pt and Pd are well established as efficient catalysts for VOCs combustion [2–4]. However, for obvious reasons, cheaper catalytic materials, involving base metal oxides, are of ever increasing importance. Thus, efforts have been made to develop transition metal based catalysts with high catalytic activity [5].

Recently, metal oxide based catalysts such as Cr_2O_3, Co_3O_4 and CuO [6–10] are increasingly applied in combustion systems in order to reduce costs associated to catalyst invention. Several studies have shown that manganese oxides MnO_2, Mn_3O_4 and α-Mn_2O_3, absorb oxygen in oxidizing atmospheres, are active and stable catalysts for the combustion of VOCs [11–15]. Among metal oxides, it is well known that ceria is a structural promoting component. It enhances the metal dispersion and participates in stabilization of the support against thermal sintering [16,17]. And ceria based catalysts for environmental purposes due to the unusual redox behavior of ceria and its high oxygen storage/transport capacity (OSC) [18].

Moreover, the choice of support is also important, as support materials play important roles in efficiency improvement of the catalyst by providing large pores and surface areas to disperse the active particles, particularly in oxidation reactions [19,20]. Pillared clays (PILCs) are considered to be a new generation of materials with a microporous three-dimensional structure of molecular dimensions [21]. PILCs have increased surface area, pore volume, thermal stability, and (depending on the pillars) improved catalytic activity compared to the parent clays, making them suitable catalysts, ion exchangers, and adsorbents [22]. PILCs are usually adopted as supports in order to maintain favorable dispersion of active metal to achieve valid utilization [23–26], particularly in environmental-friendly reactions. PILCs as catalyst supports for VOCs deep oxidation have been widely used. Some reported studies of the catalysts supported on PILCs for VOC catalytic oxidation have focused on transition metals, especially on Mn based catalysts [11,13]. These catalysts gave VOC combustion efficiencies comparable to those reported for noble catalysts and exhibited a very good stability.

The aim of our present work was to determine the most active metal/Al-PILC catalysts, and to investigate the effect of Ce added to

* Corresponding author. Tel.: +86 571 88273290; fax: +86 571 88273283.
E-mail address: zhourenxian@zju.edu.cn (R. Zhou).

0926-3373/$ – see front matter © 2009 Elsevier B.V. All rights reserved.
doi:10.1016/j.apcatb.2009.05.025

metal oxide supported on Al-PILC for deep benzene oxidation. The characterization of catalysts was performed by X-ray powder diffraction (XRD), N_2 adsorption and H_2 temperature programmed reduction (H_2-TPR) techniques.

2. Experimental

2.1. Catalysts preparation

2.1.1. Starting material

The starting material for the pillaring procedure was the sodium form of a calcium montmorillonite with a formula of $Na_{0.02}K_{0.02}Ca_{0.39}[Fe_{0.45}Mg_{1.10}Al_{2.51}][Si_{7.91}Al_{0.09}]O_{20}(OH)_4{\cdot}nH_2O$ (>100 mesh, Neimenggu, China). Al-pillaring solution aged at 60 °C for 8 h was synthesized and Al-PILC was prepared following a procedure similar to that described by our previous work [27].

2.1.2. Catalysts synthesis

M/Al-PILC catalysts were prepared by the method of incipient wetness impregnation of Al-PILC, using the corresponding nitrate salts ($Cr(NO_3)_3{\cdot}9H_2O$, $Mn(NO_3)_2$ (50%), $Fe(NO_3)_3{\cdot}9H_2O$, $Co(NO_3)_2{\cdot}6H_2O$, $Ni(NO_3)_2{\cdot}6H_2O$, $Cu(NO_3)_2{\cdot}3H_2O$ and $Ce(NO_3)_3{\cdot}6H_2O$) as precursor compounds. MCe/Al-PILC catalysts with molar ratio of Mn/Ce (6/1) were prepared by co-impregnation of Al-PILC with an aqueous solution of M and Ce nitrates. MnCe/Al-PILC catalysts were prepared with different molar ratios of Mn/Ce (3/1, 6/1, 9/1, 12/1, 18/1, 24/1 and 36/1). The impregnated samples were kept at room temperature for 12 h. Then the samples were dried at 110 °C, and subsequently calcined at 400 °C for 2 h. The total loadings of metals were 8 wt.% for all the catalysts.

2.2. Characterizations

Phase composition of samples was determined by means of XRD using Rigaku D/max-3BX. Operating parameters are as follows: monochromatic Cu Kα radiation, Ni filter, 40 mA, 40 kV.

The specific surface areas (S_{BET}), total pore volumes, micropore volumes (V_{mic}) and mesopore area (A_{mes}) of the samples were determined by nitrogen physisorption at 77 K using a Coulter OMNISORP-100 apparatus. The samples were outgassed in vacuum $<10^{-5}$ Torr at 250 °C during 2 h prior to nitrogen physicsorption.

H_2-TPR measurements were carried out on CHEMBET-3000 (Quantachrome, USA) instrument to observe reducibility of the catalysts. Prior to H_2-TPR measurement, 50 mg catalyst was pretreated at 300 °C in air for 0.5 h. The reductive gas was a mixture of 5 vol.% H_2 in Ar (40 ml/min), which was purified using deoxidizer and silica gel. Temperature of the sample was programmed to rise at a constant rate of 10 °C/min. Amount of hydrogen uptakes during the reduction was measured by a thermal conductivity detector, and the effluent H_2O formed during H_2-TPR was absorbed with a 5 A molecular sieve.

2.3. Catalytic activity tests

Benzene oxidation was carried out in a microreactor (quartz glass; 6 mm i.d., 8 mm o.d., WFS -3010, China) under atmospheric pressure at a space velocity of 20,000 h^{-1}. The reactive flow (125 ml/min) was composed of air and gaseous benzene (130–160 ppm). Catalyst (0.3–0.35 g) was loaded in the quartz reactor with quartz wool packed at both ends of the catalyst bed, and the bed volume was about 0.375 ml. A thermocouple was placed in the center of catalyst bed to record reaction temperature and also to control the furnace. Benzene conversion in the effluent gas was analyzed by on-line gas chromatography with a SE-30 (0.53 mm; 30 m) capillary column and a flame ionization detector (FID).

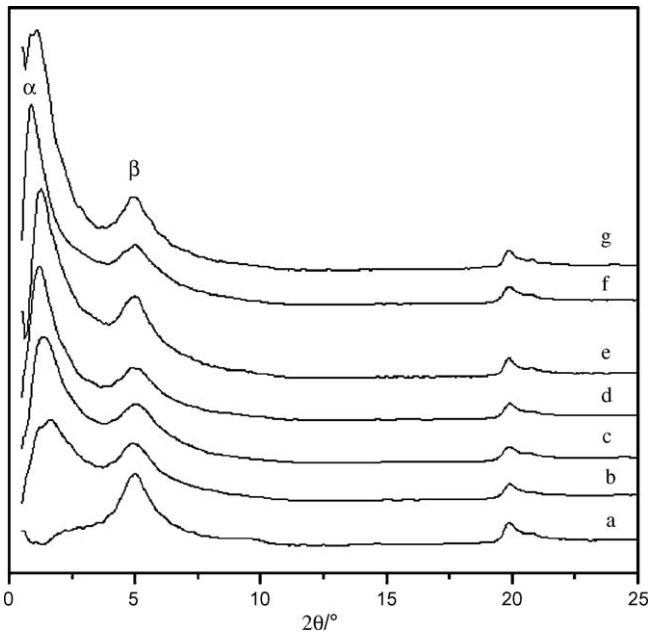

Fig. 1. XRD patterns of the catalysts between 0.5° and 25°: (a) Al-PILC; (b) CuCe (6:1)/Al-PILC; (c) CrCe (6:1)/Al-PILC; (d) MnCe (6:1)/Al-PILC; (e) NiCe (6:1)/Al-PILC; (f) FeCe (6:1)/Al-PILC; (g) CoCe (6:1)/Al-PILC.

3. Results and discussion

3.1. XRD

Fig. 1 shows the XRD patterns of MCe (6:1)/Al-PILC between 0.5° and 25°. Table 1 gives the basal spacing data and value ratios of peak α/peak β. The values of peak β (d_{001}) of MCe/Al-PILC were similar to that of Al-PILC, which indicates that the layered structure is well preserved. It is interesting that, after impregnating transition metals and Ce, a peak was observed between 2θ angles of 0.84° and 1.62°, and what's more, value ratios of peak α/peak β were about 3, 4, 5 and 6. Based on our previous research [27], it could be deduced that four, five, six and seven orderly arranged clay layers formed a super structure. We considered that some M and Ce cations migrated to hexagonal Si–O cavities within the interlayer space of Al-PILC [28,29]. After calcination, the migrated M and Ce cations were converted to MO_x and CeO_2, thus resulted in a disordered structure of some clay layers and a super structure. And the super structure could strengthen the interaction between the active species and the support.

In order to obtain the surface phases of metal oxide on Al-PILC, MCe (6:1)/Al-PILC were characterized by XRD between 20° and 80°, as presented in Fig. 2. The phases of Cr_2O_3, Fe_3O_4, Co_3O_4, NiO and CuO were observed in the corresponding catalysts, while no diffraction peaks of any manganese oxide phase in MnCe/Al-PILC

Table 1
XRD patterns and value ratios of peak α/peak β of the samples calcined at 500 °C for 2 h.

Samples	Peak α, 2θ/d (nm)	Peak β, 2θ/d_{001} (nm)	Value ratios of peak α/peak β
Al-PILC	–	4.97/1.78	–
CrCe (6:1)/Al-PILC	1.36/8.82	5.02/1.76	5.0
MnCe (6:1)/Al-PILC	1.18/7.48	4.90/1.80	4.1
FeCe (6:1)/Al-PILC	0.84/10.5	4.96/1.78	5.9
CoCe (6:1)/Al-PILC	0.98/9.0	4.92/1.79	5.0
NiCe (6:1)/Al-PILC	1.24/7.12	4.96/1.78	4.0
CuCe (6:1)/Al-PILC	1.62/5.45	4.90/1.80	3.0

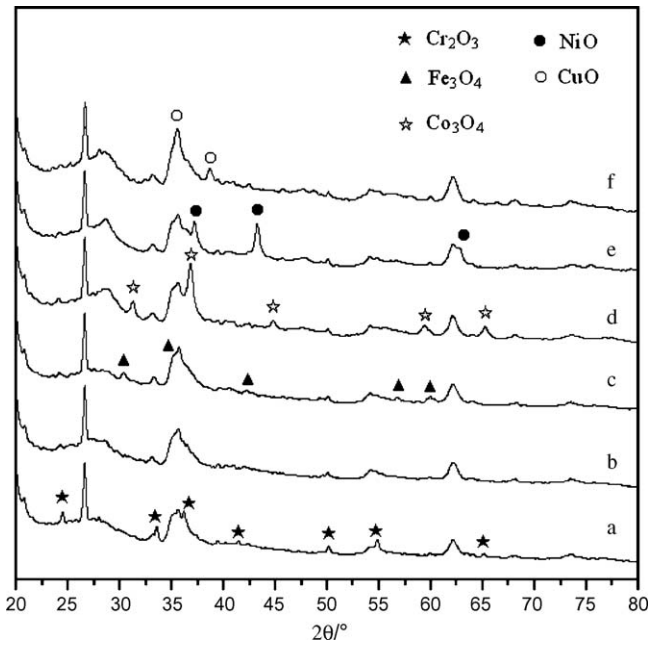

Fig. 2. XRD patterns of the catalysts between 20° and 80°: (a) CrCe (6:1)/Al-PILC; (b) MnCe (6:1)/Al-PILC; (c) FeCe (6:1)/Al-PILC; (d) CoCe (6:1)/Al-PILC; (e) NiCe (6:1)/Al-PILC; (f) CuCe (6:1)/Al-PILC.

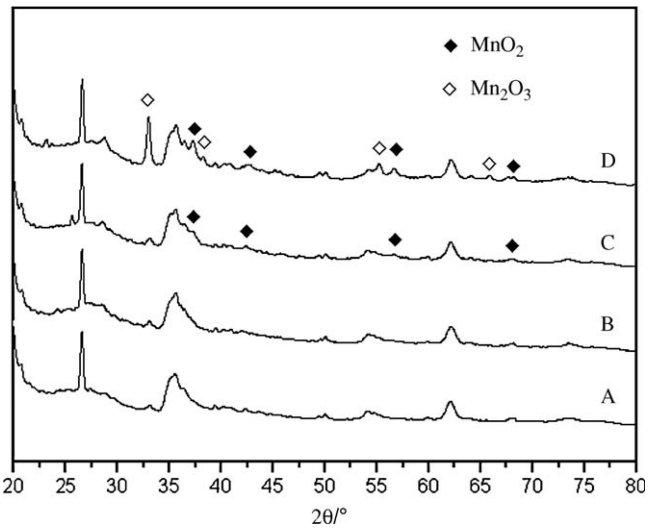

Fig. 3. XRD patterns of Al-PILC and Mn based catalysts with different Mn/Ce molar ratios between 20° and 80°: (A) Al-PILC; (B) MnCe (6:1)/Al-PILC; (C) MnCe (18:1)/Al-PILC; (D) Mn/Al-PILC.

were detected, which is probably due to the high dispersion of the supported phase over Al-PILC. The results suggest that the effect of adding Ce into M/Al-PILC is discrepant among the catalysts and Ce addition greatly improves the dispersion of MnO_x on Al-PILC.

To investigate the effect of different Ce content on the dispersion of MnO_x particles on Al-PILC, Al-PILC and a series of Mn based catalysts with different Mn/Ce molar ratios were characterized by XRD between 20° and 80°, as presented in Fig. 3. The phases of MnO_2 and Mn_2O_3 were observed for Mn/Al-PILC. For MnCe (18:1)/Al-PILC, the phase of MnO_2 was observed while no Mn_2O_3 was detected. Moreover diffraction intensity of MnO_2 was weaker than that of Mn/Al-PILC. It can be concluded for MnCe (18:1)/Al-PILC more manganese oxide species exists in higher oxidation states and that the dispersion of MnO_2 is improved after adding Ce. Compared with Al-PILC, no additional peaks characteristic of manganese oxide phases were detected for MnCe (6:1)/Al-PILC, revealing that dispersion of MnO_x increases with increasing Ce content.

3.2. N_2 adsorption

Table 2 summarized the data of textural properties of Al-PILC, Mn/Al-PILC and MnCe/Al-PILC. Doping with Mn and Ce resulted in a decrease in surface area and pore volume, and the loss of pore volume was proved that the doped cations entered into the micropores and mesopores of the Al-PILC and thus caused a reduction in V_{mic} and A_{mes} [30]. For MnCe/Al-PILC with different Mn/Ce molar ratios, Ce content increasing gave rise to a further loss of the surface area, total pore volume, A_{mes} and V_{mic}, which may be due to the fact that more Ce^{3+} with larger radius entered into the clay layers and resulted in pore blocking. But it is worth noting that, MnCe/Al-PILC (Mn/Ce > 18) had more surface area, total pore volume and A_{mes} compared to those of Mn/Al-PILC, which may be caused by the fact that the effect of the total number of ions (including Mn^{2+} and Ce^{3+}) was bigger than that of mean ion size on the textural properties. As discussed above, the textural characterization results suggested that some Mn^{2+} and Ce^{3+} reached the inner porous network of Al-PILC, resulting in a stronger interaction among MnO_x, CeO_2 and Al-PILC.

3.3. Catalytic activity

To survey the most active catalyst among (Cr, Mn, Fe, Co, Ni, Cu, Ce)/Al-PILC, deep oxidation reactions of benzene were performed, as shown in Fig. 4. In the case of Ce/Al-PILC, Cu/Al-PILC and Ni/Al-PILC, the conversions were negligibly low and they were less than 95% even at a reaction temperature of 500 °C. In the case of Mn/Al-PILC, Co/Al-PILC and Cr/Al-PILC, the conversions were 52.7%, 30.6% and 26.4%, respectively, at a reaction temperature of 320 °C and more than 98% at a reaction temperature of 400 °C. The activity of

Table 2
Surface area, pore volume and mean pore diameter of the samples calcined at 500 °C for 2 h.

Samples	Surface area (m^2/g)	Total pore volume (cm^3/g)	A_{mes}[a] (m^2/g)	V_{mic}[b] (cm^3/g)	d[c] (nm)
Al-PILC	242.5	0.171	94.4	0.067	2.94
Mn/Al-PILC	206.9	0.129	80.5	0.050	2.49
MnCe (36:1)/Al-PILC	209.6	0.134	87.3	0.059	2.56
MnCe (24:1)/Al-PILC	208.4	0.132	86.2	0.053	2.53
MnCe (18:1)/Al-PILC	208.7	0.131	86.5	0.050	2.51
MnCe (12:1)/Al-PILC	202.6	0.130	83.7	0.048	2.57
MnCe (9:1)/Al-PILC	197.7	0.127	81.8	0.046	2.57
MnCe (6:1)/Al-PILC	192.3	0.125	78.9	0.045	2.60
MnCe (3:1)/Al-PILC	182.5	0.120	72.8	0.042	2.63

[a] Mesopore surface area.
[b] Micropore volume.
[c] Mean diameter of the pores, derived from the ratio of the total pore volume to the surface area.

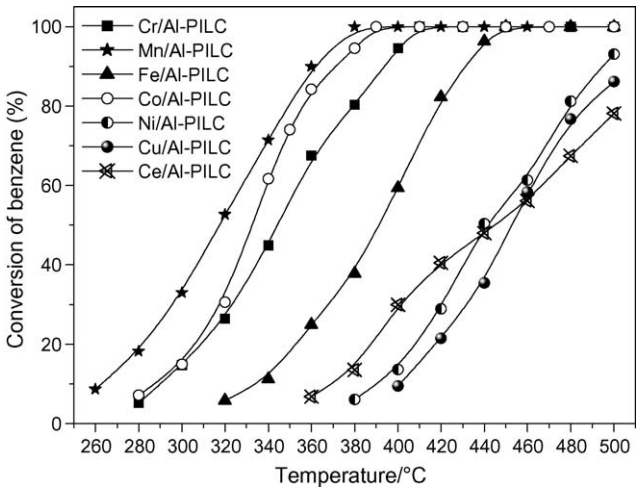

Fig. 4. Light-off curves for benzene deep oxidation over M/Al-PILC.

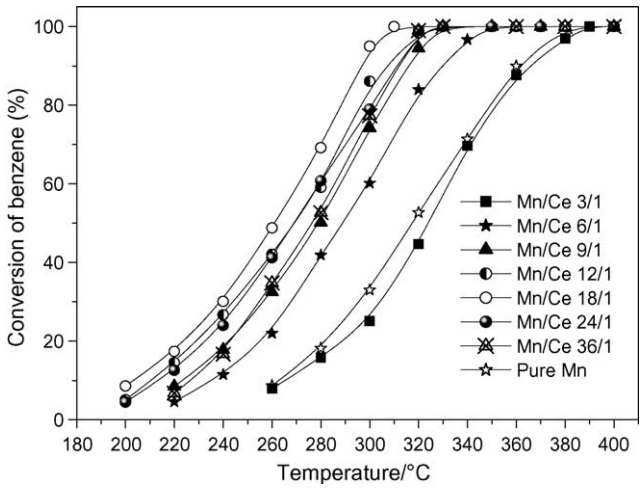

Fig. 6. Effect of Mn/Ce molar ratios on benzene deep oxidation over MnCe/Al-PILC.

M/Al-PILC with respect to metal was observed to follow the sequence: Mn > Co > Cr > Fe > Ni > Cu > Ce.

Fig. 5 shows light-off curves for benzene deep oxidation over MCe (6:1)/Al-PILC. Adding Ce obviously improved the activity of M/Al-PILC. For Cu/Al-PILC and Ni/Al-PILC, the conversions were more than 98% at a reaction temperature of 500 °C. For MnCe/Al-PILC, CrCe/Al-PILC, CoCe/Al-PILC and FeCe/Al-PILC, the conversions were 84%, 78.3%, 43.9% and 8.2%, respectively, at a reaction temperature of 320 °C. Temperature for complete oxidation of benzene with the catalyst of MnCe/Al-PILC was about 340 °C, exhibiting the highest catalytic activity. As Mn based catalysts appeared to be the most active metal, in our further research, we focused on Mn based catalyst system in the complete oxidation of benzene.

It is well known that CeO_2 enhances the oxygen storage capacity of catalysts, due to its particular ability to undergo deep and rapid reduction/oxidation cycles according to the reaction $CeO_2 \leftrightarrow CeO_{2-x} + (x/2)\ O_2$ upon interaction with reducing or oxidizing agents present in the reaction conditions [17,31–33]. When associated with transition metal oxides, CeO_2 is shown to promote oxygen storage and release, to enhance oxygen mobility to form surface and bulk vacancies, and to improve the catalyst redox properties. Addition to Mn oxide of small amounts of CeO_2 was shown to affect remarkably the oxidation state of Mn [34]. In this research, it can be summarized that introduction of Ce into M/Al-PILC improves the dispersion of transition metals, especially for Mn based catalyst, and the results were well-demonstrated by means of XRD analyses. Adding Ce induces the formation of anionic vacancies which increases the ability of the catalysts to accumulate oxygen and improves an oxygen exchange at low temperatures. So during the reaction process, CeO_2 could provide the active oxygen species to metal oxide, thus enhancing the oxidation ability of metal oxide.

Fig. 6 shows the effect of Mn/Ce molar ratios on benzene deep oxidation over MnCe/Al-PILC. From the results we deduce that Mn/Ce molar ratios have a significant impact on the catalytic activity of MnCe/Al-PILC. The catalysts exhibited a relatively low activity when Mn/Ce ratio <6, and the activity of MnCe (3:1)/Al-PILC was even lower than that of Mn/Al-PILC, which is caused by the fact that Mn is the active species while Ce acts as a promoting component. The catalyst activity was slightly decreased when Mn/Ce molar is >18, which is due to the fact that decrease of the amount of CeO_2 results in the lack of oxygen vacancies. Therefore, proper Ce content is one of the key factors to improve the MnCe/Al-PILC activity. In particular, MnCe (18:1)/Al-PILC exhibited the highest activity, and the temperature for the complete benzene conversion using this catalyst was about 310 °C.

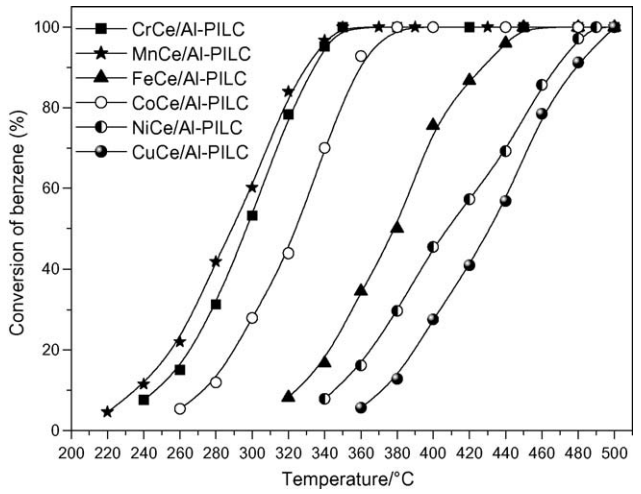

Fig. 5. Light-off curves for benzene deep oxidation over MCe (6:1)/Al-PILC.

3.4. Stability tests

The evolution with 30 h time-on-stream of benzene conversion at 340 °C for Mn/Al-PILC, at 320 °C for MnCe (6:1)/Al-PILC and at 300 °C for MnCe (18:1)/Al-PILC is reported in Fig. 7. As it can be seen, during the first 3 h on-stream all the catalysts showed a noticeable increase of the benzene conversion to reach a maximum value, and the conversion values for all the catalysts fitted in qualitatively with the catalytic performance established on the basis of the light-off experiments. MnCe/Al-PILC catalysts exhibited a relatively good maintenance of the catalytic performance. In contrast, a slow decrease of the benzene conversion took place in the case of Mn/Al-PILC catalyst. The results show that CeO_2 is doped into the MnO_x catalysts, resulting in the obvious improvement of the stability for catalytic oxidation of benzene.

3.5. H_2-TPR

H_2-TPR has been described as a sensitive technique for studying reducibility and has been applied successfully for the characterization of several catalytic systems [35]. Fig. 8 shows H_2-TPR

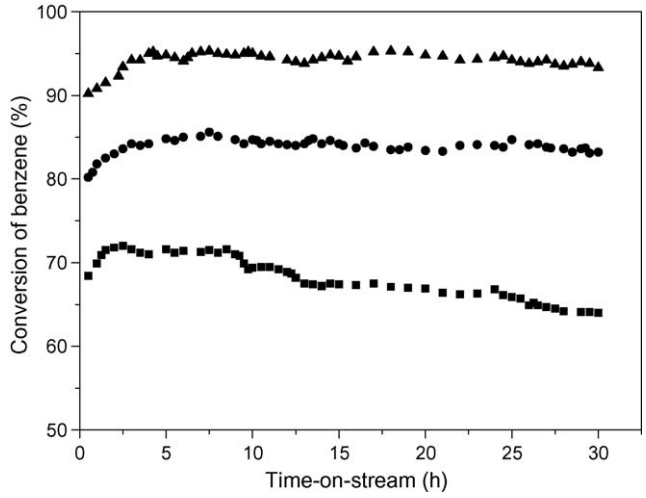

Fig. 7. Evolution of benzene conversion with time-on-stream for Mn/Al-PILC [■] at 340 °C, MnCe (6:1)/Al-PILC [●] at 320 °C and MnCe (18:1)/Al-PILC [▲] at 300 °C.

profiles of MnCe/Al-PILC with different Mn/Ce molar ratios. No significant reduction processes took place in the case of Al-PILC support (not shown). The reduction of Mn/Al-PILC started at about 200 °C and two strong overlapped reduction peaks at 371 and 455 °C were observed. Kapteijn et al. [36,37] and Boot et al. [38] reported that for the catalysts prepared from impregnation with Mn(II) nitrate solutions, both MnO_2 and Mn_2O_3 were reduced, without intermediate transformation, first in one step to Mn_3O_4 and in a second step to MnO. In our case, we found that an O/Mn stoichiometry for Mn/Al-PILC from TPR was about 1.6, which is between those of MnO_2 and Mn_2O_3 and suggests a relatively high presence of Mn_2O_3 in the catalyst. The presence of MnO_2 and Mn_2O_3 was well-demonstrated by means of XRD analyses. TPR profile of Ce/Al-PILC shows two reduction peaks at 526 and 756 °C, similar to the reported results [32,39], and these two peaks are attributed to the reduction of surface and bulk lattice oxygen, respectively.

Compared with Mn/Al-PILC, the reduction peaks of MnCe/Al-PILC with different Mn/Ce ratios systematically shifted to lower

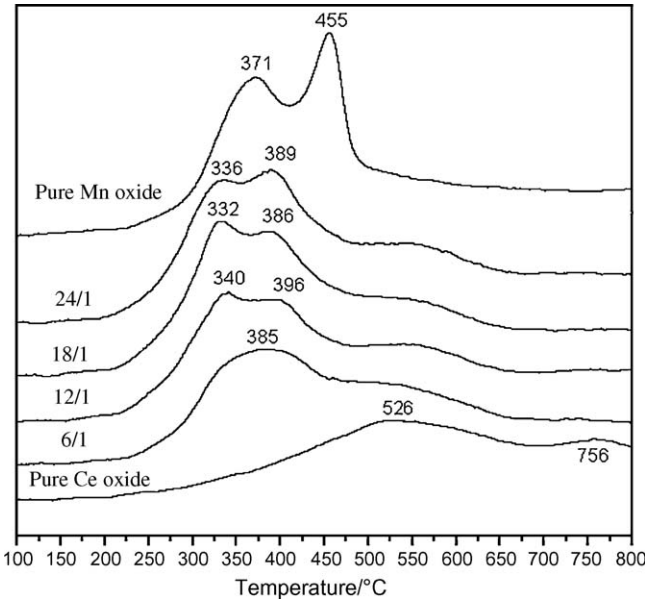

Fig. 8. TPR profiles for MnCe/Al-PILC with different Mn/Ce ratios. Consecutively from bottom to top, supported samples are: pure Ce oxide, Mn/Ce 6/1, Mn/Ce 12/1, Mn/Ce 18/1, Mn/Ce 24/1 and pure Mn oxide (Mn_2O_3 and MnO_2).

temperatures, indicating that, on one hand, Mn oxides with higher dispersion and smaller crystal size are easily reduced; on the other hand, Ce addition can change the redox properties of Mn oxide and make it easier to be reduced by the interaction between the two oxides, increasing lattice oxygen lability [40] with the promotion of the oxidation activity. As mentioned above, the first reduction peak accounts for the reduction of both MnO_2 and Mn_2O_3 to Mn_3O_4, and the second one for the reduction of Mn_3O_4 to MnO. Taking into account that the manganese oxidation state changes in each step, it can be deduced that as the MnO_2/Mn_2O_3 ratio increases, the area ratio of the first reduction peak to second also increases [24]. In our research, we found that the area ratio of first to second peak increased after adding Ce, revealing that more manganese oxide species are in higher oxidation states [13,41]. Especially for MnCe (18:1)/Al-PILC with the highest catalytic activity, the area ratio of first to second peak was highest and the temperatures of reduction peaks were lowest among the catalysts. So we conclude that trend of the area ratio of first to second peak and the reduction temperatures are related to catalyst oxidation activity. That is, MnCe/Al-PILC catalysts with higher manganese oxide state and lower reduction temperature in TPR experiment have higher catalytic activities. The intensities and areas of the reduction peaks decreases with increasing Ce content, accordingly indicating that these peaks should mainly correspond to the reduction of manganese oxide species. For MnCe (6:1)/Al-PILC, the reduction peaks of MnO_x were completely overlapped due to low Mn content. However, area of its reduction peak was bigger than that of MnCe (12:1)/Al-PILC, which suggests that the reduction temperature of surface oxygen of CeO_2 is greatly decreased owing to the strong interaction between MnO_x and CeO_2, and thus the reduction peak of CeO_2 is likely to be covered by the reduction peak of MnO_x.

4. Conclusions

In this work, transition metals and Ce supported on Al-PILC were prepared and used as catalysts for deep oxidation of low concentrations of benzene. XRD results show that a super structure was observed after impregnating transition metals and Ce on Al-PILC, which strengthens the interaction between the active species and the support. The effect of Ce addition into M/Al-PILC was discrepant among the catalysts and greatly improved the dispersion of MnO_x on Al-PILC. The results of N_2 adsorption reveal that some Mn^{2+} and Ce^{3+} reached the inner porous network of Al-PILC, resulting in a stronger interaction among MnO_x, CeO_2 and Al-PILC. TPR patterns show that Ce addition could change the redox properties of Mn oxide and make it easier to be reduced by the interaction between the two oxides, increasing lattice oxygen lability with the promotion of the oxidation activity. Activity tests in deep oxidation of low concentration of benzene show that Mn based catalysts appeared to be the most active metal and adding Ce obviously improved the activity of M/Al-PILC. Stability tests show that adding Ce could obviously improve the stability of Mn/Al-PILC for catalytic oxidation of benzene.

Acknowledgements

We gratefully acknowledge the financial supports from the Ministry of Science and Technology of China (no. 2004 CB 719504) and Nature Science Foundation of China (no. 20577043).

References

[1] M. Labaki, S. Siffert, J.-F. Lamonier, E.A. Zhilinskaya, A. Aboukaïs, Appl. Catal. B 43 (2003) 261–271.
[2] P. Papaefthimiou, T. Ionnides, X.E. Verykios, Appl. Catal. B 13 (1997) 175–184.
[3] M. Guinet, P. Dégé, P. Magnoux, Appl. Catal. B 20 (1999) 1–13.
[4] P. Papaefthimiou, T. Ioannides, X.E. Verykios, Catal. Today 54 (1999) 81–92.

[5] S.C. Kim, J. Hazard. Mater. 91 (2002) 285–299.
[6] L.C.A. Oliveira, R.M. Lago, J.D. Fabris, K. Sapag, Appl. Clay Sci. 39 (2008) 218–222.
[7] H. Rotter, M.V. Landau, M. Carrera, D. Goldfarb, M. Herskowitz, Appl. Catal. B 47 (2004) 111–126.
[8] J. Li, Z. Mu, X. Xu, H. Tian, M. Duan, L. Li, Z. Hao, S. Qiao, G. Lu, Microporous Mesoporous Mater. 114 (2008) 214–221.
[9] C. Mazzocchia, A. Kaddouri, J. Mol. Catal. A 204–205 (2003) 647–654.
[10] L. Storaro, R. Ganzerla, M. Lenarda, R. Zanoni, A.J. López, P. Olivera-Pastor, E.R. Castellón, J. Mol. Catal. A 115 (1997) 329–338.
[11] L.M. Gandía, M.A. Vicente, A. Gil, Appl. Catal. B 38 (2002) 295–307.
[12] D. Döbber, D. Kiebling, W. Schmitz, G. Wendt, Appl. Catal. B 52 (2004) 135–143.
[13] A. Gil, M.A. Vicente, S.A. Korili, Catal. Today 112 (2006) 117–120.
[14] X. Tang, Y. Xu, W. Shen, Chem. Eng. J. 144 (2008) 175–180.
[15] T. Mishra, P. Mohapatra, K.M. Parida, Appl. Catal. B 79 (2008) 279–285.
[16] R. Dictor, S. Roberts, J. Phys. Chem. 93 (1989) 5846–5850.
[17] A. Martinez-Arias, M. Fernández-García, L.N. Salamanaca, R.X. Valenzuela, J.C. Conesa, J. Soria, J. Phys. Chem. B 104 (2000) 4038–4046.
[18] A. Trovarelli, M. Boaro, E. Rocchini, C. De Leitenburg, G. Dolcetti, J. Alloys Compd. 323 (2001) 584–591.
[19] K. Okumura, T. Kobayashi, H. Tanaka, M. Niwa, Appl. Catal. B 44 (2003) 325–331.
[20] W. Lin, L. Lin, Y. Zhu, Y. Xie, K. Scheurell, E. Kemnitz, J. Mol. Catal. A 226 (2005) 263–268.
[21] A. Gil, M.A. Vicente, L.M. Gandía, Microporous Mesoporous Mater. 34 (2000) 115–125.
[22] T.J. Pinnavaia, Science 220 (1983) 365–371.
[23] K. Narui, H. Yata, K. Furuta, A. Nishida, Y. Kohtoku, T. Matsuzaki, Appl. Catal. A 179 (1995) 165–173.
[24] L.M. Gandía, M.A. Vicente, A. Gil, Appl. Catal. A 196 (2000) 281–292.
[25] L. Yang, C. Shi, X. He, J. Cai, Appl. Catal. B 38 (2002) 117–125.
[26] N. Marín-Astorga, G. Alvez-Manoli, P. Reyes, J. Mol. Catal. A 226 (2005) 81–88.
[27] S. Zuo, R. Zhou, Microporous Mesoporous Mater. 113 (2008) 472–480.
[28] R. Tettenhorst, Am. Miner. 47 (1962) 769–773.
[29] N.D. Hutson, D.J. Gualdoni, R.T. Yang, Chem. Mater. 10 (1998) 3707–3715.
[30] H.Y. Zhu, Z.H. Zhu, G.Q. Lu, J. Phys. Chem. B 104 (2000) 5674–5680.
[31] M.A. Centeno, M. Paulis, M. Montes, J.A. Odriozola, Appl. Catal. A 234 (2002) 65–78.
[32] H.C. Yao, Y.F. Yu Yao, J. Catal. 86 (1984) 254–265.
[33] T. Miki, T. Ogawa, M. Haneda, N. Kakuta, A. Ueno, S. Tateishi, S. Matsuura, S. Sato, J. Phys. Chem. 94 (1990) 6464–6474.
[34] S. Imamura, M. Schnono, N. Okamoto, S. Hamada, S. Ishida, Appl. Catal. A 142 (1996) 279–288.
[35] A. Jones, B. McNicol, Temperature-Programmed Reduction for Solids Materials Characterization, Marcel Dekker, New York, 1986.
[36] F. Kapteijn, A. Dick van Langeveld, J.A. Moulijn, A. Andreïni, M.A. Vuurman, A.M. Turek, J.-M. Jehng, I.E. Wachs, J. Catal. 150 (1994) 94–104.
[37] F. Kapteijn, L. Singoredjo, A. Andreïni, J.A. Moulijn, Appl. Catal. B 3 (1994) 173–189.
[38] L.A. Boot, M.H.J.V. Kerkhoffs, B.Th. van der Linden, A. Jos van Dillen, J.W. Geus, F.R. van Buren, Appl. Catal. A 137 (1996) 69–86.
[39] M. Jobbágy, F. Mariño, B. Schönbrod, G. Baronetti, M. Laborde, Chem. Mater. 18 (2006) 1945–1950.
[40] C. De Leitenburg, D. Goi, A. Primavera, A. Trovarelli, G. Dolcetti, Appl. Catal. B 11 (1996) L29–L35.
[41] H. Chen, A. Sayari, A. Adnot, F. Larachi, Appl. Catal. B 32 (2001) 195–204.